NJC

ROYAL SOCIETY OF CHEMISTRY

PAPER

View Article Online
View Journal | View Issue

Cite this: *New J. Chem.*, 2021, **45**, 3716

Synthesis, characterization and antibacterial applications of pyrazolyl-sulfonamides and their palladium complexes†

Cephas Amoah, [ab] Collins Obuah, *[ab] Michael Kojo Ainooson, [ab] Christian Kwaku Adokoh [bc] and Alfred Muller[b]

A series of pyrazolyl sulfonamide compounds were prepared by a multi-step procedure involving preparation of phenyl pyrazolyl compounds (**C1**, **C2**) and their chlorosulfonated derivatives (**C3–C5**), which were then converted to sulfonamides (**L1–L6**). Complexes of **L1–L6** with palladium(II) show the standard *trans* square-planar coordination environment for the six complexes (**1–6**). All products were prepared in moderate to high yield (61–81%). All compounds were successfully characterized by NMR spectroscopy, IR spectroscopy, mass spectrometry and in one case single X-ray crystallography. Conversion of **C1** and **C2** to **C3–C5** is governed by steric hindrance on the pyrazolyl group as sulfonation of the phenyl only is observed for ^{t}Bu groups (**C4**), whereas for Me groups sulfonation of the pyrazolyl is observed **C3** as well as phenyl ring for **C5**. Antimicrobial screening was carried out on the compounds using the agar-well diffusion method at varying concentrations of (62.5, 125, 250, 500 and 1000 μg mL^{-1}) on ten (10) bacteria strains. The zone of inhibition for all the compounds are within the ranges of 9.5 mm to 25 mm compared to the control antibiotic, gentamicin that was between 16.5 mm to 36 mm. The compounds **L1–L6** generally showed mild to strong antibacterial activity in the zones of inhibition against most Gram negative bacteria strains tested, but no activity against Gram positive bacteria strains *Staphylococcus aureus* and *Enterococcus faecalis*, except **L4** which showed activity towards *Staphylococcus*. The palladium(II) complexes generally showed improved activities for all the bacteria strains studied with **4** exhibiting the most potent *in vitro* anti-bacterial activity with MICs of 1.046 μg mL^{-1} and 0.237 μg mL^{-1} against *Staphylococcus epidermidis* and *Proteus mirabilis* respectively. Theoretical Log P calculation show values between 3.06 and 5.95 for the ligands and between 6.67 and 12.36 for complexes. Suggesting high affinity of these compounds to the lipophilic medium. However, the experimental Log P value gave a different trend, which shows that compounds with sulfonation only on the phenyl ring (**L3** (−0.83), **L4** (−0.53), **3** (−0.96) and **4** (−0.72)) have high affinity for the hydrophilic medium.

Received 19th October 2020,
Accepted 1st February 2021

DOI: 10.1039/d0nj05143h

rsc.li/njc

1. Introduction

Antibacterial resistance has become a threat to global health, food security and human development. In recent years, the rapid emergence of multidrug resistant bacteria caused by the wide application of antibiotics in clinical practices has cause great difficulties in medical treatment leading to increased mortality, higher treatment costs and increased illness recovery time.[1] The use of heterocyclic moieties have attracted significant interest and attention in the development of pharmacologically active molecules.[2,3] Pyrazole, a five membered aromatic compound as well as its derivatives have gained popularity in drug development due to its manifold use in agents such as anti-bacterial,[4] anti-microbial,[5] anticonvulsant,[6,7] anti-cancer[8,9] and anti-tubercular.[10] Sulfonamides, on the other hand are structural analogues of *para*-aminobenzoic acid (PABA) (the precursor for making folic acid), which shows varying solubility, absorption and excretion characteristics. The significance of the sulfonamide moiety in medicinal chemistry cannot be ignored as they exhibit diverse biological properties including anti-bacterial and anti-diabetic properties. According to Jain *et al.*[11] sulfonamides play an important role in the transition state mimetic of peptide hydrolysis, as a potent irreversible inhibitor of cysteine proteases

[a] *Department of Chemistry, University of Ghana, Legon, Ghana. E-mail: cobuah@ug.edu.gh*
[b] *Department of Chemical Sciences, University of Johannesburg, Auckland Park 2006, Johannesburg, South Africa*
[c] *Department of Forensic Sciences, School of Biological Sciences, University of Cape Coast, Cape Coast, Ghana*

† Electronic supplementary information (ESI) available. CCDC 2039260. For ESI and crystallographic data in CIF or other electronic format see DOI: 10.1039/d0nj05143h

during anti-microbial activities. More recently, they have also found use as anti-cancer, antiviral agents and in the treatment of Alzheimer's disease.[12] Experimental analysis has also shown that anti-microbial activities of organic ligands and their metal complexes are strongly dependent on the central metal ion.[13] Hence the emergence of some metal complexes of palladium and platinum complexes have shown appreciable activities as anti-tumor agents. This is attributed to the labile nature of these complexes compared to known compounds such as cisplatin and carboplatin.[14] Palladium, due to its similar coordination chemistry to platinum and some advantages like higher solubility of its complexes when compared to platinum, has attracted attentions as a potential candidate in drug discovery.[15–18] It has been reported that palladium(II) complexes show high cytotoxicity activity against head and neck squamous cancer, ovarian cancer, breast cancer, malignant melanoma, glioma, human colorectal adenocarcinoma, osteogenic sarcoma, human chronic myelogenous leukemia, prostate cancer, lung cancer and human cervical epithelial cancer.[19] However, the evolution of resistant strains of bacteria, viruses and fungi to commonly known biologically active agents have become a great concern in clinical medicine. For these reasons, synthesis of new chemical products are on the rise to fight these diseases and infections. A number of combinatory synthesis of very active compounds have been employed to provide a sure inhibition of resistant breeds. It is therefore well known that combination of multiple biologically active moieties in a single pharmacophore improves the bioactivity of the compound and associated resistance to the microbes.[20]

As such, this study report the synthesis of biological active scaffold comprising of the combination of sulfonamide and pyrazolyl moieties into a single pharmacophore, complexed with palladium(II) metal. The anti-bacterial activities of the ligands and palladium complexes are also reported here in.

2. Experimental section

2.1 Materials and methods

Unless otherwise stated, all manipulations were carried out under nitrogen atmosphere using standard Schlenck techniques. All organic solvents were dried and purified by distillation over standard reagents under nitrogen prior to use. Compound $[PdCl_2(NCMe)_2]$ was synthesized according to literature procedure.[21] Compounds chlorosulfonic acid, phenyl hydrazine, pentane-2,4-dione, *tert*-butylamine, propylamine and 2,2,6,6-tetramethyl-3,5-heptadione, octanol were purchased from Sigma-Aldrich. All chemicals were used as received.

Antimicrobial activity was carried out using the well diffusion method.[22] The standard bacteria strains used for the anti-microbial activity were obtained from Noguchi Memorial Institute for Medical Research, Accra, Ghana. The compounds were screened for their antimicrobial activity in triplicate, against the selected bacteria at varying concentrations of 1000, 500, 250, 125 and 62.5 μg mL^{-1}.[22] Gentamicin, used as positive control, was purchased from the pharmacy stores. All procedures employed were based on the standard operating procedure (SOP) adapted from Clinical and Laboratory Standards Institute (CLSI) of the United States of America (CLSI, 2017).[23] Bacteria strains used are: Gram-positive *Staphylococcus aureus*, *Enterococcus faecalis*, *Staphylococcus epidermidis* and Gram negative *Citrobacter freundii*, *Salmonella typhi*, *Pseudomonas aeruginosa, Vibro cholera* O1E1 Tor, *Proteus mirabilis*, *Escherichia coli* and *Klebsiella pnemoniae.*

Infrared (IR) spectra of ligands and complexes were recorded on a PerkinElmer Spectrum Two equipped with a diamond ATR. Elemental analyses were performed on a Vario Elementar III microcube CHNS. The mass spectrometry unit at the Chemistry Department, University of Cape Coast performed the ESI-MS spectra on a Waters API Qualtro micro spectrophotometer. NMR spectra were recorded on a Bruker 500 MHz instrument (^1H at 500 MHz and $^{13}C\{^1H\}$ at 125 MHz) at the Department of Chemistry, University of Ghana. The chemical shifts are reported in δ (ppm) and referenced to the residual proton and carbon signals 7.24 ppm and 77.0 ppm respectively of $CDCl_3$ NMR solvent.

2.1.1 Preparations of test compounds (pyrazolyl sulfonamides) for anti-microbial screening. Test ligands and complexes were prepared through a serial dilution (1000, 500, 250, 125 and 62.5 μg mL^{-1}) of approximately 0.01 g of individual compounds dissolved in 10 mL DMSO to obtain a stock concentration of 1000 μg mL^{-1}.

2.1.2 Gram staining. Individual organisms were sub cultured on nutrient agar with each bacterial cell smeared on a slide and heat fixed. Crystal violet (primary stain) was added onto the slide for a minute and gently rinse with running tap water to remove excess crystal violet. Subsequently, iodine (mordant) was added for a minute and rinse with acetone for 30 seconds. Then, Safranin was added for a minute and rinse with running tap water. The slide was viewed under an electron microscope to establish the virility of the bacteria strains.

2.1.3 Preparations of sub-cultures from control strains. The control strains; *Staphylococcus aureus* (ATCC 25923), *Klebsiella pnuemoniae* (ATCC 43816), *Citrobacter freundii* (ATCC43864), *Escherichia coli* (ATCC 25922), *Salmonella typhi* (ATCC 19430), *Staphylococcus epidermidis* (ATCC 12228), *Pseudomonas aeruginosa* (ATCC 15442), *Proteus mirabilis* (ATCC 25933), *Vibro cholerae* (ATCC 39451) and *Enterococcus faecalis* (ATCC 9790) were kept at −80 °C and thawed before use. Nutrient agar plates were prepared and a loop full of control bacteria strains spread over the surface of the agar-based nutrient medium in quadrants so that bacterial cells are deposited at widely separated points on the surface of the medium. All the procedures were aseptically performed, by flaming both the loop and rim of the bottle or tube, before and after removing the inoculum. The plates were then incubated upside-down for 24 h.[23]

2.1.4 Preparation of inoculum and media. The sub cultured test organisms were transferred into 0.1% sterile peptone water *via* a sterile inoculating loop and emulsified to 0.5 MacFarland standard. Prior to antibiotic susceptibility testing, the bacterial suspensions were incubated at 37 °C for 10 to 15 mins in a bacteriological incubator.

A Mueller-Hinton (MH) agar, for Antibiotic Susceptibility Testing (AST) was prepared according to the manufacturer's instructions (Microgen, Central Drug 40 House LTD, New Delhi – India).

2.1.5 Test procedure. The well diffusion technique was used according to National Committee for Clinical Laboratory Standards (NCCLS) for AST using Muller Hinton medium plates. Inoculum containing 106 cfu per mL of each bacterium to be tested was spread on the plates with a sterile swab moistened with the bacterial suspension.[24] Subsequently, wells of 6 mm diameter were punched into the agar medium and filled with two drops of each test compounds with different concentrations. Wells containing the same volume of two percent concentrated DMSO and distilled water served as negative controls while standard gentamycin drug was used as the positive control. Three replicates were carried out for each drug against each of the test organisms. Plates were then incubated at 37 °C for 18–24 h in a bacteriological incubator. Zones of inhibition of the various compounds were measured to the nearest millimeters (mm).

2.1.6 Determination of the minimum inhibition concentration. The zones of inhibition, X, was measured for each concentration of gentamicin and the novel compounds as shown in the eqn (1).[24]

$$X = (a - b)/2 \quad (1)$$

where X = zone of inhibition, a = inhibition zone diameter and b = diameter of wells.

The diameter of inhibition zone was determined to be directly proportional to concentration of drugs. A graph relation of X^2 against the log of concentration was plotted to obtain the intercept of the various drug action. Anti-log of the x intercept was then calculated to obtain the MIC of the drug compounds as reported in literature.[25]

2.1.7 Theoretical calculation of the lipophilicity or hydrophilicity of the compounds using their relative solubility Log *P* values. The solubility profile of all tested compounds were estimated using atom/fragment contribution method that predicts $\log P_{calc}$.[26] The solubility contributions (groups and substituents) are expressed as hydrophilic negative value or lipophilic (positive value) fragment constants as shown in eqn (2).[26]

$$\text{Log}\, P_{calc.} = \sum\chi \quad (2)$$

where $\text{Log}\, P_{calc}$ = log of partition coefficient and $\sum\chi$ = sum of hydrophilic or lipophilic constants.

2.1.8 Experimental Log *P* estimation. In determining the Log *P* of the ligands (**L1–L6**) and metal complexes (**1–6**), the traditional shake-flask method was employed at a temperature of 298 K. An aqueous phase adjusted with phosphate buffer at pH 7.4 was used whilst 1-octanol was used as the organic phase. Equal amounts of the both phases were combined and kept for saturation for 24 hours. Known amounts of the compounds were dissolved in equal amounts of the aqueous and octanol phases, shaken and left for separation for 24 h. The concentration of the compounds in the aqueous and octanol phase were determined using analytical UV method from developed calibration curves (Fig. S31–S35, ESI†). The Log *P* was calculated as the log of the ratio of the concentration of the compound in the octanol phase to the concentration in the aqueous phase at pH 7.4.

2.1.9 Statistical analysis. All data were entered into a spreadsheet of Microsoft Excel and transferred to a graph pad prism. This was done to present the results in tables and graph charts for the analysis of the inhibition zones and to compute the minimum inhibition concentration of the drugs.

2.2 Synthesis of ligands

2.2.1 Synthesis of 3,5-dimethyl-1-phenyl-1*H*-pyrazole (C1). An ethanol solution (20 mL) of pentane-2,4-dione (5.45 g, 0.05 mol) was added to a stirring ethanol solution (30 mL) of phenyl hydrazine (5.05 g, 0.05 mol). The resultant mixture was refluxed at 80 °C for 12 h to give an orange solution. This solution was evaporated to afford analytically pure dark orange oil. Yield = 6.98 g (81%). ^{1}H NMR ($CDCl_3$): δ 2.27 (s, 3H, CH_3); 2.28 (s, 3H, CH_3); 5.97 (s, 1H, pz-H); 7.33 (m, 1H, Ph); 7.42 (m, 4H, Ph). $^{13}C\{^1H\}$ NMR ($CDCl_3$): δ 12.2; 13.41; 106.8; 124.6; 127.1; 128.8; 139.2; 139.8. GCMS (EI) m/z $[M]^+$ calcd 172.100: found: 172.152 (100%).

Compound **C2** was prepared in a similar manner as described for **C1**, using appropriate reagents.

2.2.2 Synthesis of 3,5-di-*tert*-butyl-1-phenyl-1*H*-pyrazole (C2). The compound 2,2,6,6-tetramethylheptane-3,5-dione (0.92 g, 5.0 mmol) was reacted with phenyl hydrazine (0.54 g, 5.0 mmol) to give light brown solid. Yield = 0.83 g (65%). ^{1}H NMR, ($CDCl_3$): δ 1.14 (s, 9H, ^{t}Bu); 1.31 (s, 9H, ^{t}Bu); 5.98 (s, 1H, pz-H); 7.37 (m, 1H, Ph); 7.40 (m, 4H, Ph). $^{13}C\{^1H\}$ NMR ($CDCl_3$): δ 30.6; 30.8; 100.2; 128.5; 128.7; 129.0. GCMS (EI) m/z $[M]^+$ calcd 256.190: found: 256.182 (100%).

2.2.3 Synthesis of 3,5-dimethyl-1-phenyl-1*H*-pyrazole-4-sulfonyl chloride (C3). Solution of compound **C1** (1.85 g, 11.0 mmol) was added slowly to an excess chlorosulfonic acid while stirring under ice bath. This dark solution was stirred under ice bath for 30 min and further refluxed for 2 h. The resulting mixture was poured into ice and the product extracted with chloroform. The extract was evaporated to obtain a brown oil. Yield = 2.23 g (77%). ^{1}H NMR ($CDCl_3$): δ 2.53 (s, 3H, CH_3); 2.54 (s, 3H, CH_3); 7.39 (d, 2H, $^3J_{HH}$ = 8.5 Hz, Ph); 7.53 (m, 3H, Ph); $^{13}C\{^1H\}$ NMR ($CDCl_3$): δ 12.0;13.1; 122.8; 125.7; 129.5; 137.6. GCMS (EI) m/z $[M]^+$ calcd: 270.020; found; 270.150 (100%).

Compounds **C4** and **C5** were prepared in a similar manner as described for **C3**, using the appropriate reagents.

2.2.4 Synthesis of 4-(3,5-di-*tert*-butyl-1*H*-pyrazol-1-yl)benzene-1-sulfonyl chloride (C4). Compound **C2** (0.73 g, 2.8 mmol) was added to chlorosulfonic acid to obtain a light brown oil. Yield = 0.82 g (81%). ^{1}H NMR, ($CDCl_3$): δ 1.15 (s, 9H, ^{t}Bu); 1.52 (s, 9H, ^{t}Bu); 6.25 (s, 1H, pz-H); 7.43 (m, 1H, $^3J_{HH}$ = 8.0 Hz, Ph); 7.65 (d, 2H, $^3J_{HH}$ = 7.0 Hz, Ph); 7.73 (s, 1H, Ph). $^{13}C\{^1H\}$ NMR ($CDCl_3$): δ 29.65; 29.73; 29.91; 32.25; 32.72; 102.73; 126.18; 126.78; 128.61; 128.88; 130.30; 133.92; 146.38; 158.99. GCMS (EI) m/z $[M]^+$ calcd: 354.120; found: 354.250 (100%).

2.2.5 Synthesis of 1-(4-(chlorosulfonyl)phenyl)-3,5-dimethyl-1*H*-pyrazole-4-sulfonyl chloride (C5). Compound **C1** (0.7 g, 4.1 mmol) was added to chlorosulfonic acid to obtain a brown

oil which solidifies after 3 days. Yield = 1.06 g (71%). ^{1}H NMR ($CDCl_3$): δ 2.55 (s, 3H, CH_3); 2.64 (s, 3H, CH_3); 2.67 (s, 3H, CH_3); 7.73 (d, 1H, $^3J_{HH}$ = 8.5 Hz, Ph); 7.83 (d, 1H, $^3J_{HH}$ = 5.0 Hz, Ph); 8.16 (s, 1H, Ph); 8.22 (d, 1H, $^3J_{HH}$ = 8.5 Hz, Ph). $^{13}C\{^1H\}$ NMR ($CDCl_3$): δ 12.1; 12.3; 13.0; 13.1; 123.9; 126.2; 127.4; 128.5; 131.1; 131.6; 138.7. GCMS (EI) m/z = $[M]^+$ calcd 367.950; found: 368.012 (100%).

2.2.6 Synthesis of *N*-(*tert*-butyl)-3,5-dimethyl-1-phenyl-1*H*-pyrazole-4-sulfonamide (L1). To a 10 mL CH_2Cl_2 solution of 3,5-dimethyl-1-phenyl-1*H*-pyrazole-4-sulfonyl chloride (**C3**) (0.41 g, 1.5 mmol) was added *tert* butylamine in a 1 : 1 mole ratio and the resulting solution stirred at 50 °C for 3 h. The solvent was evaporated to afford analytically pure dark brown oil. The compound was purified by column chromatography, using a solvent system of a mixture of ethyl acetate–hexane in a 10 : 1 ratio. The purified product was oily but solidifies after a few hours. Yield = 0.36 g (77%). ^{1}H NMR ($CDCl_3$): δ 1.26 (s, 9H, ^{t}Bu); 2.44 (s, 3H, CH_3); 2.45 (s, 3H, CH_3); 7.34 (d, 2H, $^3J_{HH}$ = 8.5 Hz, Ph); 7.42 (t, 1H, $^3J_{HH}$ = 5.0 Hz, Ph); 7.46 (t, 2H, $^3J_{HH}$ = 8.5 Hz, Ph). $^{13}C\{^1H\}$ NMR ($CDCl_3$): δ 11.8; 13.0; 27.3; 29.9; 54.4; 120.17; 125.7; 128.7; 129.2; 138.3; 141.6. IR (Diamond ATR, cm^{-1}): 3254 ν(N–H) amine. GCMS (EI) m/z $[M]^+$ calcd 307.140; found: 307.135 (100%). Anal. calcd for $C_{15}H_{21}N_3O_2S$: C, 58.61; H, 6.89; N, 13.67; S, 10.43%. Found: C, 58.82; H, 7.01; N, 13.41; S, 10.72%. Calculated log $P_{o/w}$: 3.44; experimental Log $P_{o/w}$: 1.01.

Compounds **L2–L6** were prepared in a similar manner as described for **L1**, using the appropriate reagents.

2.2.7 Synthesis of *N*-(propyl)-3,5-dimethyl-1-phenyl-1*H*-pyrazole-4-sulfonamide (L2). A CH_2Cl_2 solution of 3,5-dimethyl-1-phenyl-1*H*-pyrazole-4-sulfonyl chloride (**C3**) (0.55 g, 2.0 mmol) was added to propylamine to afford a light brown oil, which solidifies after few hours. Yield = 0.47 g (79%). ^{1}H NMR ($CDCl_3$): δ 0.91 (t, 3H, $^3J_{HH}$ = 7.5 Hz, CH_3); 1.54 (m, 2H, $^3J_{HH}$ = 7.0 Hz, CH_2); 2.45 (s, 3H, CH_3); 2.46 (s, 3H, CH_3); 2.94 (m, 2H, $^3J_{HH}$ = 7.0 Hz, CH_2); 4.41 (s, 1H, NH); 7.36 (d, 2H, $^3J_{HH}$ = 7.0 Hz, Ph); 7.43 (t, 1H, Ph); 7.48 (t, 2H, Ph). $^{13}C\{^1H\}$ NMR ($CDCl_3$): δ 11.18; 11.86; 13.13; 22.87; 44.48; 116.87; 125.70; 128.86; 129.31; 138.38; 142.60. IR (Diamond ATR, cm^{-1}): 3278 ν(N–H) amine. GCMS (EI) m/z $[M]^+$ calcd: 293.120; found: 293.119 (100%). Anal. calcd for $C_{14}H_{19}N_3O_2S$: C, 57.31; H, 6.53; N, 14.32; S, 10.93%. Found C, 57.52; H, 6.80; N, 14.91; S, 10.62%. Calculated log $P_{o/w}$: 3.16; experimental Log $P_{o/w}$: 2.96.

2.2.8 Synthesis of *N*-(*tert*-butyl)-4-(3,5-di-*tert*-butyl-1*H*-pyrazol-1-yl)benzenesulfonamide (L3). A 20 mL CH_2Cl_2 solution of 4-(3,5-di-*tert*-butyl-1*H*-pyrazol-1-yl)benzene-1-sulfonyl chloride (**C4**) (0.51 g, 1.4 mmol) was added to *tert*-butylamine to afford a dark brown oil, which solidifies after few hours. Yield = 0.498 g (81%). ^{1}H NMR ($CDCl_3$): δ 1.12 (s, 9H, CH_3); 1.21 (s, 9H, CH3); 1.27 (s, 9H, CH_3); 4.08 (s, 1H, NH); 5.98 (s, 1H, pz-H); 7.75 (d, 1H, Ph); 7.82 (s, 1H, Ph); 7.89 (m, 2H, Ph). $^{13}C\{^1H\}$ NMR ($CDCl_3$): δ 27.59; 28.66; 30.44; 32.86; 33.53; 52.49; 100.64; 106.92; 126.4; 128.8; 129.03; 130.33; 130.89; 142.2. IR (Diamond ATR, cm^{-1}): 3415 ν(N–H) amine. GCMS (EI) m/z $[M - Me]^+$ calcd: 377.210; found: 377.250 (100%). Anal. calcd for $C_{21}H_{33}N_3O_2S$: C, 64.41; H, 8.49; N, 10.73; S, 8.19%. Found C, 64.60; H, 8.54; N, 10.86; S, 8.33%. Calculated log $P_{o/w}$: 5.95; experimental Log $P_{o/w}$: −0.83.

2.2.9 Synthesis of 4-(3,5-di-*tert*-butyl-1*H*-pyrazol-1-yl)-*N*-propylbenzenesulfonamide (L4). A 20 mL CH_2Cl_2 solution of 4-(3,5-di-*tert*-butyl-1H-pyrazol-1-yl)benzene-1-sulfonyl chloride (**C4**) (0.22 g, 0.6 mmol) was added to propylamine to afford a dark brown oil, which solidifies after few hours. Yield = 0.177 g (76%). ^{1}H NMR ($CDCl_3$): δ 0.87 (t, 3H, $^3J_{HH}$ = 7.5 Hz, CH_3); 1.13 (s, 9H, CH3); 1.22 (s, 6H, CH_3); 1.26 (d, 7H, CH_3); 1.35 (s, 5H, CH_3); 1.61 (m, 2H, CH_2); 2.83 (m, 2H, $^3J_{HH}$ = 7.5 Hz, CH_2); 5.99 (s, 1H, pz-H); 7.76 (d, 1H, Ph); 7.83 (d, 1H, Ph); 7.92 (m, 2H, Ph). $^{13}C\{^1H\}$ NMR ($CDCl_3$): 10.74; 20.72; 30.35; 30.37; 30.46; 30.79; 31.82; 31.86; 32.79; 33.48; 41.53; 100.63; 106.88; 126.44; 128.8; 130.28; 130.77; 144.72; 153.51; 155.83. IR (Diamond ATR, cm^{-1}): 3428 ν(N–H). GCMS (EI) $m/z[M]^+$ calcd: 377.210; found: 377.257 (100%). Anal. calcd for $C_{20}H_{31}N_3O_2S$: C, 63.63; H, 8.28; N, 11.13; S, 8.49%. Found C, 63.71; H, 8.44; N, 11.40; S, 8.80%. Calculated log $P_{o/w}$: 5.77; experimental Log $P_{o/w}$: −0.53.

2.2.10 Synthesis of *N*-(*tert*-butyl)-1-(4-(*N*-(*tert*-butyl)sulfamoyl)phenyl)-3,5-dimethyl-1H-pyrazole-4-sulfonamide (L5). A CH_2Cl_2 solution of 1-(4-(chlorosulfonyl)phenyl)-3,5-dimethyl-1*H*-pyrazole-4-sulfonyl chloride (**C5**) (0.34 g, 0.9 mmol) was added to *tert*-butylamine in a ratio of 1 : 2 to afford a bright brown oil, which solidifies after few hours. Yield = 0.28 g (71%). ^{1}H NMR ($CDCl_3$): δ 1.22 (s, 9H, CH_3); 1.26 (s, 9H, CH3); 2.45 (s, 3H, CH_3); 2.50 (s, 3H, CH_3); 4.86 (d, 1H, NH); 5.03 (d, 1H, NH); 7.51 (d, 1H, $^3J_{HH}$ = 9.0 Hz, Ph); 7.58 (m, 1H, Ph); 7.91 (t, 1H, Ph); 8.04 (d, 1H, Ph). $^{13}C\{^1H\}$ NMR ($CDCl_3$): δ 11.90; 12.06; 13.10; 14.13; 20.98; 29.69; 30.11; 30.13; 54.59; 54.97; 55.08; 60.35; 121.41; 123.85; 125.64; 126.77; 128.13; 129.07; 130.05; 138.92; 141.30; 141.72; 141.75. IR (Diamond ATR, cm^{-1}): 3276 ν(N–H) amine. GCMS (EI) m/z $[M]^+$ calcd:442.170; found: 442.544 (100%). Anal. calcd for $C_{19}H_{30}N_4O_4S_2$: C, 51.56; H, 6.83; N, 12.66; S, 14.49%. Found C, 51.76; H, 6.99; N, 12.78; S, 14.61%. Calculated log $P_{o/w}$: 3.41; experimental Log $P_{o/w}$: 0.94.

2.2.11 Synthesis of 3,5-dimethyl-*N*-propyl-1-(4-(*N*-propylsulfamoyl)phenyl)-1*H*-pyrazole-4-sulfonamide (L6). A CH_2Cl_2 solution of 1-(4-(chlorosulfonyl)phenyl)-3,5-dimethyl-1*H*-pyrazole-4-sulfonyl chloride (**C5**) (0.37g, 1.0 mmol) was added to propylamine in a ratio of 1 : 2 mole to afford a bright brown oil, which solidifies after few hours. Yield = 0.34 g (83%). ^{1}H NMR ($CDCl_3$): δ 0.89 (m, 6H, CH_3); 1.51 (m, 4H, CH_2); 2.45 (s, 3H, CH_3); 2.51 (s, 3H, CH_3); 2.94 (m, 4H, CH_2); 4.71 (t, 1H, NH); 4.77 (t, 1H, NH); 7.55 (d, 1H, $^3J_{HH}$ = 6.5 Hz, Ph); 7.62 (m, 1H, Ph); 7.91 (t, 1H, $^3J_{HH}$ = 5.0 Hz, Ph); 7.98 (d, 1H, $^3J_{HH}$ = 6.5 Hz, Ph). $^{13}C\{^1H\}$ NMR ($CDCl_3$): δ 10.96; 11.10; 11.87; 12.02; 13.06; 13.08; 22.85; 22.93; 22.95; 44.44; 44.95; 45.00; 124.08; 125.75; 126.91; 128.23; 129.25; 130.15; 140.19. IR (Diamond ATR, cm^{-1}): 3292 ν(N–H) amine. GCMS (EI) m/z $[M]^+$ calcd: 414.140; found: 414.141 (100%). Anal. Calcd for $C_{17}H_{26}N_4O_4S_2$: C, 49.25; H, 6.32; N, 13.52; S, 15.47%. Found: C, 49.51; H, 6.71; N, 13.80; S, 15.54%. Calculated log $P_{o/w}$: 3.06; experimental Log $P_{o/w}$: 0.67.

2.3 Synthesis of complexes

2.3.1 Synthesis of dichloro-bis-*N*-(*tert*-butyl)-3,5-dimethyl-1-phenyl-1*H*-pyrazole-4-sulfonamide pallidum(II) complex (1). To a 10 mL MeOH solution of (0.46 g, 1.5 mmol) *N*-(*tert*-

butyl)-3,5-dimethyl-1-phenyl-1*H*-pyrazole-4-sulfonamide (**L1**) was added to (0.19 g, 0.7 mmol) $[Pd(MeCN)_2Cl_2]$ precursor as prepared in literature[21] and the resulting solution stirred at room temperature for 5 h. The solvent was evaporated and the complex formed precipitated after a CH_2Cl_2 solution was layered with hexane. Further recrystallization were done to afford a pure complex. Yield = 0.49 g (83%). ^{1}H NMR ($CDCl_3$): δ 1.56 (s, 18H, CH_3); 2.30 (s, 6H, CH3); 2.36 (s, 6H, CH_3); 4.42 (s, 2H, NH); 7.36 (d, 2H, $^3J_{HH}$ = 8.5 Hz, Ph); 7.67 (m, 10H, Ph). $^{13}C\{^1H\}$ NMR ($CDCl_3$): δ 11.9; 13.5; 29.86; 55.0; 121.5; 129.4; 129.9; 130.8; 136.3; 145.4; 150.5. IR (Diamond ATR, cm^{-1}): 3280 ν(N–H) amine. GCMS (EI) m/z $[M]^+$ calcd: 790.110; found: 790.148 (80%). Anal. calcd for $C_{30}H_{42}Cl_2N_6O_4PdS_2$: C, 45.49; H, 5.34; N, 10.61; S, 8.10%. Found: C, 45.67; H, 5.51; N, 10.70; S, 8.42%. Calculated log $P_{o/w}$: 7.05; experimental Log $P_{o/w}$: 1.20.

Compounds **2–6** were prepared in a similar manner as described for **1**, using the appropriate reagents.

2.3.2 Synthesis of dichloro-bis-*N*-(propyl)-3,5-dimethyl-1-phenyl-1*H*-pyrazole-4-sulfonamide pallidum(II) complex (2). To a MeOH solution of (0.44 g, 1.50 mmol) *N*-(propyl)-3,5-dimethyl-1-phenyl-1*H*-pyrazole-4-sulfonamide (**L2**) was added to (0.19 g, 0. 7 mmol) $[Pd(MeCN)_2Cl_2]$. Yield = 0.46 g (81%). ^{1}H NMR ($CDCl_3$): δ 0.88 (t, 6H, $^3J_{HH}$ = 7.5 Hz, CH_3); 1.49 (m, 4H, $^3J_{HH}$ = 7.0 Hz, CH_2); 2.30 (s, 6H, CH_3); 2.36 (s, 6H, CH_3); 2.88 (m, 4H, $^3J_{HH}$ = 7.0 Hz, CH_2); 4.35 (t, 2H, NH); 7.69 (s, 10H, Ph). $^{13}C\{^1H\}$ NMR ($CDCl_3$): δ 11.0; 12.0; 13.6; 22.81; 44.4; 118.8; 129.5; 129.8; 130.9; 146.0; 150.8. IR (Diamond ATR, cm^{-1}): 3265 ν(N–H) amine. GCMS (EI) m/z $[M + H]^+$ calcd: 762.080; found: 762.148 (65%). Anal. calcd for $C_{17}H_{26}N_4O_4S_2$: C, 49.25; H, 6.32; N, 13.52; S, 15.47%. Found C, 49.51; H, 6.71; N, 13.80; S, 15.54%. Calculated log $P_{o/w}$: 6.69; experimental Log $P_{o/w}$: 3.23.

2.3.3 Synthesis of dichloro-bis-*N*-(*tert*-butyl)-4-(3,5-di-*tert*-butyl-1*H*-pyrazol-1-yl)benzenesulfonamide palladium(II) complex (3). To a 10 mL MeOH solution of (0.25 g, 0.6 mmol) *N*-(*tert*-butyl)-4-(3,5-di-*tert*-butyl-1*H*-pyrazol-1-yl)benzenesulfonamide (**L3**) was added to (0.08 g, 0.3 mmol) $[Pd(MeCN)_2Cl_2]$. Yield = 0.19 g (62%). ^{1}H NMR ($CDCl_3$): δ 1.15 (d, 18H, CH_3); 1.22 (d, 18H, CH_3); 1.78 (m, 9H, CH_3); 1.99 (m, 9H, CH_3); 4.12 (m, 1H, NH); (m, 1H, NH); 6.10 (s, 2H, Pz); 7.77 (m, 2H, Ph); 7.89 (m, 2H, Ph); 8.59 (m, 4H, Ph). $^{13}C\{^1H\}$ NMR ($CDCl_3$): δ 27.79; 29.68; 29.98; 30.13; 31.3; 32.6; 33.6; 53.5; 108.1; 127.3; 129.9; 132.0; 142.4; 144.8. IR (Diamond ATR, cm^{-1}): 3445 ν(N–H) amine. GCMS (EI) m/z $[M]^+$ calcd: 958.300; found: 958.311 (75%). Anal. calcd for $C_{42}H_{66}Cl_2N_6O_4PdS_2$: C, 52.52; H, 6.93; N, 8.75; S, 6.68%. Found C, 52.70; H, 7.01; N, 8.65; S, 6.81%. Calculated log $P_{o/w}$: 12.36; experimental Log $P_{o/w}$: −0.96.

2.3.4 Synthesis of dichloro-bis-4-(3,5-di-*tert*-butyl-1*H*-pyrazol-1-yl)-*N*-propylbenzenesulfonamide palladium(II) complex (4). To a 10 mL MeOH solution of (0.22 g, 0.6 mmol) 4-(3,5-di-*tert*-butyl-1*H*-pyrazol-1-yl)-*N*-propyl benzenesulfonamide (**L4**) was added to (0.08 g, 0.3 mmol) $[Pd(MeCN)_2Cl_2]$. Yield = 0.17 g (61%). ^{1}H NMR ($CDCl_3$): δ 0.86 (t, 12H, CH_3); 1.19 (m, 9H, CH_3); 1.23 (m, 9H, CH_3); 1.65 (d, 4H, $^3J_{HH}$ = 7.5 Hz, CH_2); 1.80 (m, 9H, CH_3); 2.02 (m, 9H, CH_3); 2.93 (s, 4H, CH_2); 6.07 (m, 2H, Pz); 7.63 (m, 2H, Ph); 7.91 (m, 2H, Ph); 7.91 (s, 2H, Ph); 8.33 (m, 2H, Ph). $^{13}C\{^1H\}$ NMR ($CDCl_3$): δ 10.88; 13.98; 20.74; 22.53; 29.86; 30.05; 31.46; 41.89; 108.1; 127.3; 129.9; 132.0; 142.4; 144.8. IR (Diamond ATR, cm^{-1}): 3459 ν(N–H). GCMS (EI) m/z $[M]^+$ 930.270; found: 930.280 (80%). Anal. calcd for $C_{40}H_{62}Cl_2N_6O_4PdS_2$: C, 51.53; H, 6.70; N, 9.01; S, 6.88%. Found C, 51.79; H, 6.66; N, 9.25; S, 6.96%. Calculated log $P_{o/w}$: 12.00; experimental Log $P_{o/w}$: −0.72.

2.3.5 Synthesis of dichloro-bis-*N*-(*tert*-butyl)-1-(4-(*N*-(*tert*-butyl)sulfamoyl)phenyl)-3,5-dimethyl-1*H*-pyrazole-4-sulfonamide palladium(II) complex (5). To a 10 mL MeOH solution of (0.37 g, 0.8 mmol) *N*-(*tert*-butyl)-1-(4-(*N*-(*tert*-butyl)sulfamoyl)phenyl)-3,5-dimethyl-1*H*-pyrazole-4-sulfonamide (**L5**) was added to (0.11 g, 0.4 mmol) $[Pd(MeCN)_2Cl_2]$. Yield = 0.35 g (78%). ^{1}H NMR ($CDCl_3$): δ 1.25 (d, 18H, CH_3); 1.34 (s, 9H, CH3); 1.35 (s, 9H, CH_3); 2.32 (m, 6H, CH_3); 2.40 (m, 6H, CH_3); 4.60 (s, 1H, NH); 4.83 (m, 3H, NH); 7.82 (d, 2H, $^3J_{HH}$ = 7.0 Hz, Ph); 7.88 (t, 1H, $^3J_{HH}$ = 8.0 Hz, Ph); 7.97 (d, 1H, Ph); 8.05 (d, 1H, Ph); 8.25 (t, 3H, Ph). $^{13}C\{^1H\}$ NMR ($CDCl_3$): δ 11.92; 29.88; 30.14; 30.22; 50.75; 128.11; 130.44. IR (Diamond ATR, cm^{-1}): 3296 ν(N–H). GCMS (EI) m/z $[M]^+$ 1060.180; found: 1060.181 (55%). Anal. calcd for $C_{38}H_{60}Cl_2N_8O_8PdS_4$: C, 42.96; H, 5.69; N, 10.55; S, 12.07%. Found C, 43.05; H, 5.73; N, 10.68; S, 12.11%. Calculated log $P_{o/w}$: 7.38; experimental Log $P_{o/w}$: 1.10.

2.3.6 Synthesis of dichloro-bis-3,5-dimethyl-*N*-propyl-1-(4-(*N*-propylsulfamoyl)phenyl)-1*H*-pyrazole-4-sulfonamide palladium(II) complex (6). To a 10 mL MeOH solution of (0.38 g, 0.9 mmol) 3,5-dimethyl-*N*-propyl-1-(4-(*N*-propylsulfamoyl)phenyl)-1*H*-pyrazole-4-sulfonamide (**L6**) was added to (0.12 g, 0.5 mmol) $[Pd(MeCN)_2Cl_2]$. Yield = 0.37 g (81%). ^{1}H NMR ($CDCl_3$): δ 0.90 (m, 12H, $^3J_{HH}$ = 6.0 Hz, CH_3); 0.95 (m, 4H, CH_2); 1.23 (s, 4H, CH_2); 2.36 (m, 12H, CH_3); 2.95 (m, 4H, $^3J_{HH}$ = 7.0 Hz, CH_2); 3.09 (m, 4H, $^3J_{HH}$ = 8.0 Hz, CH_2); 4.70 (t, 2H, NH); 4.93 (m, 2H, NH); 7.88 (m, 3H, $^3J_{HH}$ = 8.5 Hz, Ph); 8.00 (t, 2H, $^3J_{HH}$ = 7.5 Hz, Ph); 8.20 (t, 3H, $^3J_{HH}$ = 8.5 Hz, Ph). $^{13}C\{^1H\}$ NMR ($CDCl_3$): δ 11.1; 12.1; 12.3; 22.8; 23.0; 23.1; 29.6; 44.4; 44.5; 45.2; 128.18; 130.5. IR (Diamond ATR, cm^{-1}): 3283 ν(N–H) amine. GCMS (EI) m/z $[M + H]^+$ calcd: 1004.120 found; 1004.125 (60%). Anal. calcd for $C_{34}H_{52}Cl_2N_8O_8PdS_4$: C, 40.58; H, 5.21; N, 11.13; S, 12.74%. Found: C, 40.66; H, 5.49; N, 11.32; S, 12.89%. Calculated log $P_{o/w}$: 6.67; Experimental Log $P_{o/w}$: 0.91.

3. Results and discussion

3.1 Synthesis of ligands

Compounds **C1** and **C2** were prepared from the condensation reaction of phenyl hydrazine with appropriate diketones; pentane-2,4-dione in **C1** and 2,2,6,6-tetramethylheptane-3,5-dione in **C2** as reported in Scheme S1 (ESI†). They afforded a viscous dark brown oil which solidifies after some time for **C2**. The structure of these compounds were confirmed by ^{1}H NMR spectroscopy (Fig. S1 and S2, ESI†). Compounds **C3–C5** (Scheme S1, ESI†) were synthesized from the sulfonation of **C1** and **C2** with excess chlorosulfonic acid followed by extraction of the compounds from aqueous-dichloromethane solvent mixture to yield tacky brown solids which solidified after few hours. These compounds were purified by column chromatography, using a solvent system of a mixture of ethyl acetate-hexane

in a 10 : 1 ratio. The compounds were characterized by IR and NMR spectroscopies. The IR spectra revealed the absence of the pyrazolyl proton, which was not observed in the pyrazole sulfonated products but present in the phenyl sulfonated products. This is evident in the corresponding IR spectra of the ligands (Fig. S6–S8, ESI†) around 3051 cm^{-1}. In addition, the spectra of the corresponding ligands **C4** and **C5** showed C–H bending vibrations in the fingerprint region and is characteristic of di-substituted phenyls (Fig. S7 and S8, ESI†).

The ^{1}H-NMR analysis of the sulfonated products **C3–C5** showed a shift to higher frequencies compared to the starting compounds **C1** and **C2**. For example, methyl and *tert*-butyl proton peaks for **C1** and **C2** is observed at 2.26 ppm, and 1.14–1.31 ppm respectively, whiles in the sulfonated products were observed at 2.54 ppm, and 1.17–1.55 ppm (Fig. S3 and S4, ESI†) for **C3** and **C4** respectively. These observations are expected as the sulfonyl group is an electron withdrawing group. Further ^{1}H-NMR analysis on **C3–C5** (Fig. S3–S5, ESI†) confirmed the absence of the pyrazolyl proton in **C3** and **C5** and in addition substituted phenyl ring for **C4** and **C5** as predicted by the IR spectroscopy. The ^{1}H-NMR of **C3** in Fig. S3 (ESI†) showed a doublet and a triplet between 7.37 ppm and 7.52 ppm, both integrating for five protons for the phenyl group. In the case of **C4** and **C5**, four protons were observed in the spectra in the same region (Fig. S4 and S5, ESI†). From experimental observations, the sulfonation first occurs on the pyrazolyl ring before the phenyl ring if the 3,5-positions of the pyrazolyl ring has less bulky substituents. Similar observations have been made by Attaryan *et al.*[27] in which the substitution was a first to the pyrazolyl ring before the phenyl ring, thus establishing that the pyrazolyl proton is the more acidic compared to the phenyl protons in the system.

This observation differ from the known chemistry of pyrazole compounds in which the simplest route of attack is always to the substituent attached to the pyrazole but will later attack the pyrazole upon further harsh conditions such as increased temperature.[28] However, due to steric hindrance, this observation could not be made for **C4** (Fig. S4, ESI†). The ^{1}H NMR spectrum of **C4** shows distinct splitting pattern of doublets and triplets for the phenyl ring between 7.40 ppm and 7.67 ppm suggesting an aromatic substitution at the *para* position. Interestingly, ^{1}H NMR spectrum of **C5** (Fig. S5, ESI†) also showed a distinct splitting of all the phenyl protons into doublets and multiplets which suggest an *para* substitution, In all, **C3** and **C4** are mono sulfonated compounds while **C5** is a di-sulfonated compound.

Further reactions were carried on **C3–C5** with *tert*-butylamine and propylamine, in 1 : 1 mole ratio to yield **L1–L4** (Schemes 1 and 2) and 1 : 2 mole ratio to yield **L5** and **L6** (Scheme 3). The methyl substituted pyrazolyl derivatives gave oily product which solidified after few hours while the *tert*-butyl substituted pyrazolyl derivative yielded a solid product. The compounds **L1**, **L2**, **L5** and **L6** were purified by column chromatography with a solvent system of ethyl acetate-hexane in a 10 : 1 ratio while **L3** and **L4** was ethyl acetate-methanol in a 7 : 3 ratio. All synthesized ligands were observed to be very stable under ambient temperature after a long time of storage signifying a possible longer shelf life. However, ligands **L5** and **L6** were found to be hygroscopic and required to be stored under inert conditions.

Ligands **L1–L6** were characterized using ^{1}H-NMR, ^{13}C{^{1}H}-NMR, IR and GC-MS. IR spectra of compounds **L1–L6** (Fig. S6–S8, ESI†) suggest the formation of the proposed sulfonamides from the presence of characteristic secondary amine (N–H) peaks around ~3200–3450 cm^{-1}.

As expected, the ^{1}H NMR spectra of **L1–L6** (Fig. S9–S11, ESI†) showed the upfield shift of the proton peaks compared to their precursor compounds **C3–C5** due to the presence of an amine group. For example, methyl and *tert*-butyl proton peaks for precursors **C3** and **C4** are observed at 2.54 ppm, and 1.16–1.55 ppm. On the other hand, for compounds **L1** and **L3** they are observed at 2.49 ppm and 1.13–1.27 ppm (Fig. S9 and S10, ESI†). One characteristic peak which confirmed the formation of all the expected compounds is the presence of the amine proton peak which is between 4.49 ppm and 4.78 ppm. The ^{1}H-NMR data of ligands **L5** and **L6** showed a peculiar peak splitting of the pyrazolyl methyl protons. Three distinct peaks for the methyl protons was observed instead of the expected two, in a 2 : 1 ratio. (Fig. S11, ESI†). Also, ^{13}C{^{1}H}-NMR spectrum confirmed that the carbon bearing these protons showed three peaks instead of two peaks (Fig. S14, ESI†). HSQC experiment carried on **L6** demonstrated three carbons to proton correlation from the F1 and F2 axis indeed existed in the compound (Fig. S30, ESI†). The same observation was obtained for **C5** (Fig. S5, ESI†). This could be due to polymorphic behavior of the sulphonyl group. Similar observations have been reported by Koike *et al.*[29] and Nangia *et al.*[30] in which the presence of co-crystals polymorphic forms were observed in sulfathiazole-oxalic acid complex and sulfonamide with carboxamide compounds respectively. Thus, the sulfonamide point of attachment to the pyrazole in **L6** provides free movement for the sulfonamide group to flip between two forms (that is one in plane and the other out of plane), hence observed in the NMR spectrum when the pyrazolyl methyl group show 3 peaks. Therefore, it could be concluded that the presence of possible polymorphic forms of the double substituted phenylpyrazolyl sulfonamide existed in **C5** and its analogs.

GC-MS analysis on the compounds provided a further confirmation of the formation of the proposed compounds from the GC-trace and mass spectra of each compound as shown in Fig. S24–S29 (ESI†). For example, **L1** showed *m*/*z* of the molecular ion as [M^+] = 307.135 which corresponds to the

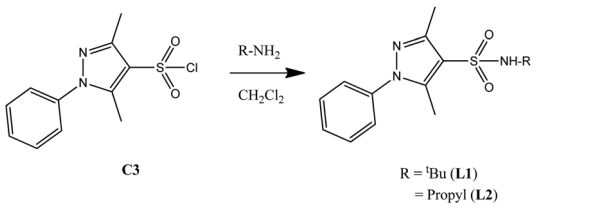

Scheme 1 Synthesis of single sulfonated phenylpyrazolyl sulfonamides.

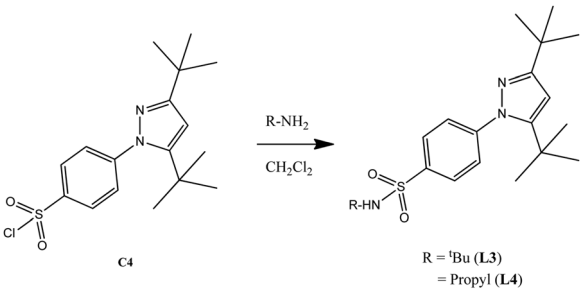

Scheme 2 Synthesis of phenyl-sulfonated pyrazolyl sulfonamides.

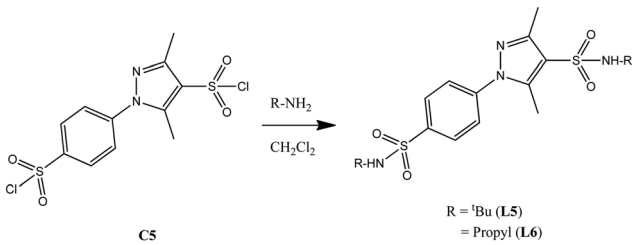

Scheme 3 Synthesis of double sulfonated phenylpyrazolyl sulfonamides.

molecular mass of the proposed compound. Compound **L3** also showed a m/z of 377.250 which correspond $[M - CH_3]^+$ while **L5** had a m/z of 442.544 which also agrees with the proposed structure. Elemental analysis was used to confirm the purity and proposed structures.

3.2 Synthesis of palladium(II) complexes

Palladium(II) precursor, $[Pd(MeCN)_2Cl_2]$ was reacted with **L1–L6** in a 2 : 1 mole ratio at room temperature to yield complexes **1–6** as depicted in Schemes 4–6. Through recrystallization in dichloromethane and hexane, complexes **1–6** were isolated as solids with a characteristic pale yellow to brown. The solubility of the complexes were found to decrease with decreasing polarity of the complexes. For example, **1** and **2** easily precipitated from methanol during the reaction while the rest were soluble.

All complexes were characterized using IR, ^{1}H NMR and $^{13}C\{^1H\}$ NMR spectroscopy. IR spectroscopy revealed a general shift of all the bands to higher wave numbers in all the complexes synthesized compared to their corresponding ligands (Fig. S9–12 and S15–S17, ESI†).

The ^{1}H-NMR and $^{13}C\{^1H\}$ NMR spectra showed a downfield shift in frequency for the various groups depending on their relative electron densities and distance from the metal center. For example, for the ^{1}H NMR of **L1** and **1**, it was observed that the addition of a metal resulted in a further shifting of the aromatic protons downfield from about 7.44 ppm to 7.66 ppm and while there was an upfield shift for the *tert*-butyl protons from 1.28 ppm to 1.21 ppm (Fig. S9 and S15, ESI†), owing to the nature of the group and point of attachment in the complex (attached to an electron rich nitrogen atom). Also, integration of the peaks of the compounds indicate there are two ligands complexes to a palladium metal. This observation could be

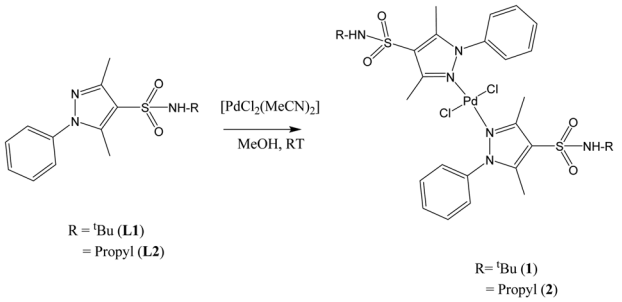

Scheme 4 Synthesis of single sulfonated phenylpyrazolyl sulfonamides palladium(II) complexes.

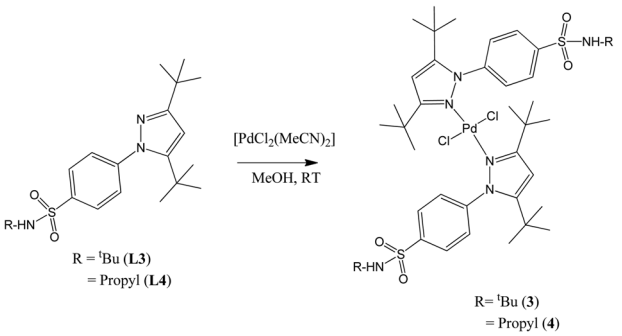

Scheme 5 Synthesis of single sulfonated phenylpyrazolyl sulfonamides palladium(II) complexes.

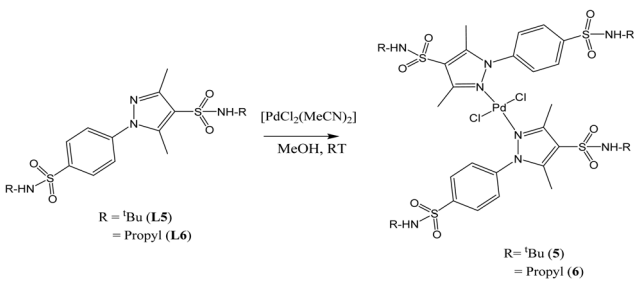

Scheme 6 Synthesis of double sulfonated phenylpyrazolyl sulfonamides palladium(II) complexes.

made for all the complexes suggesting the absence of a bridging center within them. In addition, a careful study of the pyrazolyl methyl substituent in both spectrum showed a clear splitting of what was previously observed as a singlet peak at around 2.46 ppm in **L1** with a peak integration of 6 protons, separated into two peaks (2.36 ppm and 2.29 ppm) in **1** with an integration of 3 protons for each ligand (Fig. S9 and S15, ESI†), confirming that an attachment to the nitrogen atom could possibly account for the unequal or dissimilar chemical environment for the methyl substituents. This again provides first-hand information on which nitrogen atom is involved in the metal binding. A similar observation is made for **L2** and **2** and the splitting of the 3,5-pyrazolyl substituent is well noticed in the complexes of **L5** and **L6**.

3.3 Molecular structure of 2

Single crystals suitable for X-ray analysis of **2** were obtained by slow evaporation of their CH_2Cl_2 solutions at 25 °C. Crystallographic data are tabulated in Table 1, whereas the molecular geometries and selected bond lengths and angles are presented in Fig. 1. Complex **2** crystallizes as one independent molecule in the asymmetric unit, in a monoclinic crystal system and $P2_1/c$ space group.

The crystal structures of **2** showed slightly distorted square planar geometries about the palladium centre with bond angles between 88.74(9)–91.26(9)°. The smallest N–Pd–Cl angles are 88.74(9)°, whereas the largest N–Pd–Cl angles are 91.26(9)°. The Pd–N bond lengths of **2** (1.999(3) Å), is somewhat shorter than the Pd–N bond lengths found in pyrazolyl palladium complexes that have Pd–N($_{pz}$) bonds where they range from 2.034(3) to 2.060(3) Å,[31,32] and the Pd–Cl bond lengths of **2** (2.2936(9) Å), is in the normal range (2.242–2.516 Å) as 1776 palladium complexes to which two nitrogen atoms and two chloride ions are ligated to the palladium that are reported in the Cambridge Structural Database (CSD).[33]

3.4 Antimicrobial activity

3.4.1 Anti-microbial activities of sulfonamide pyrazolyl compounds against both Gram-negative & positive bacteria. The pyrazolyl sulfonamide ligands (**L1–L6**) and their palladium complexes (**1–6**) were dissolved in DMSO and the resulting solutions screened for their antimicrobial activity against seven Gram negative bacteria; *Citrobacter freundii* (ATCC43864), *Escherichia coli* (ATCC 25922), *Salmonella typhi* (ATCC 19430), *Proteus mirabilis* (ATCC 25933), *Vibro cholerae* (ATCC 39451), *Klebsiella pnuemoniae* (ATCC 43816) and three Gram positives; *Staphylococcus aureus* (ATCC 25923), *Enterococcus faecalis* (ATCC 9790) and *Staphylococcus epidermidis* (ATCC 12228). These microbes are human pathogenic bacteria that tend to cause wide range of infections including urinary tract infections, intestinal infections and respiratory tract infections. Also, they can develop certain resistant strategies such as inactivation of antimicrobial agents and modification of microbial target within the host organism, which impedes the activity of drug

Table 1 Crystal data and structure refinement for complex **2**

	2
Empirical formula	$C_{14}H_{19}ClN_3O_2Pd_{0.5}S$
Formula weight	382.03
Temperature/K	100.01
Wavelength/Å	0.71073
Crystal system	Monoclinic
Space group	$P2_1/c$
a/Å	11.6678(17)
b/Å	8.0747(12)
c/Å	17.753(3)
α/(°)	90
β/(°)	93.372(4)
γ/(°)	90
Volume (Å^3)	1669.7(4)
Z	4
Density (Mg m^{-3})	1.520
Final R indices [$I > 2\mathrm{sigma}(I)$]	R_1 = 0.0507, wR_2 = 0.1121

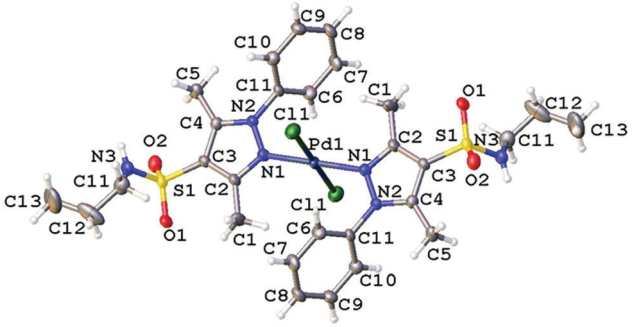

Fig. 1 A molecular drawing of **2** with 50% probability ellipsoids. Selected bond lenght [Å] and angles [°]: Pd1–Cl1, 2.2936(9); Pd1–N1, 1.999(3); N1–N2, 1.369(4); C3–S1, 1.744(3); S1–O2, 1.429(3); S1–O1, 1.427(3); S1–N3, 1.625(3); Cl1^1–Pd1–Cl1, 180.0; N1–Pd1–Cl1, 88.74(9);N1^1–Pd1–Cl1, 91.26(9); S1–N3–C15, 116.9(3).

or antimicrobial agent[34] and expulsion of antimicrobial agents from the bacterial cell to survive within the host.[35] It has become imperative for new formulation be made to overcome their resistance. For this study, gentamicin, the standard antibiotic, was used as a positive control with DMSO as solvent. The well diffusion method was employed for the antimicrobial sensitivity test, which provides accurate and reproducible results as well as good aseptic methods as prescribed by the WHO.[36] The growth inhibitions as well as the minimum inhibition concentration (MIC) values were determined for concentrations of 62.5, 125, 250, 500 and 1000 μg mL^{-1}. Table S1 (ESI†) presents the zones of inhibition of the test compounds for these concentrations. The compounds generally exhibited mild to strong antibacterial activities as shown in zones of inhibition against mostly Gram negative bacteria strains tested. The zone of inhibition for all the compounds fell within the ranges of 9.5 mm to 25 mm and that of the control antibiotic gentamicin was between 16.5 mm to 36 mm for low dosage of 62.5 μg mL^{-1} to high dosage of 1000 μg mL^{-1}. The highest concentration (1000 μg mL^{-1}) recorded the highest zone of inhibition of all the tested compounds. The control antibiotic gentamicin showed maximum activity against all selected microbes with zones of inhibition ranging between 16.5-36 mm at 1000 μg mL^{-1}. However, all the ligands showed no activity against Gram positive bacteria strains *Staphylococcus aureus* and *Enterococcus faecalis*, except **L4** which showed activity for *Staphylococcus aureus* within the zone inhibition comparable to the standard test drug Gentamicin (Table S1: entries 4 and 13, ESI†). Also, trends similar to the observed activity for the ligands could be made for their palladium complexes except for **1** and **4** (Table S1: entries 7 and 10, ESI†). The most significant observation made is that the addition of palladium to the ligands improved the activities of some compounds. For example, compound **L1** was not active against *Staphylococcus aureus* but its palladium adduct showed good activity comparable to the standard drug (Table S1 entries 1, 7 and 13, ESI†). Complex **4** showed improved zone inhibition activity compared to it ligand **L4** (Table S1: entries 4 and 10, ESI†). Complexes **1** and **4** showing activities towards

Table 2 Minimum inhibition concentrations (μg mL^{-1}) of tested compounds for both Gram positive and Gram negative bacteria

Entry	Compound	*S. aureus*	*S. epidermidis*	*E. faecalis*	*E. coli*	*P. aeruginosa*	*V. cholerae*	*S. typhii*	*C. freundiii*	*K. pneumoniae*	*P. mirabilis*
1	**L1**	—	32.58	—	10.79	9.55	42.46	7.64	3.83	47.86	10.69
2	**L2**	—	7.24	—	5.23	7.12	13.06	4.92	21.23	34.83	—
3	**L3**	—	—	—	27.35	—	15.92	14.50	14.43	46.88	—
4	**L4**	—	23.01	—	—	—	—	—	—	46.70	—
5	**L5**	—	60.67	—	—	>1000	55.59	—	—	—	>1000
6	**L6**	—	—	—	64.41	6.40	—	10.19	8.51	>1000	—
7	**1**	—	3.36	—	5.12	6.52	7.98	—	—	9.05	3.64
8	**2**	—	1.61	—	3.66	4.88	8.46	3.26	10.25	4.30	—
9	**3**	—	—	—	10.55	—	9.31	12.01	11.23	31.21	—
10	**4**	—	1.05	—	41.59	33.73	32.30	—	—-	21.35	0.237
11	**5**	—	40.23	—	—	>1000	32.56	—	—	—	>1000
12	**6**	—	—	—	20.58	4.69	—	8.64	7.01	>1000	—
13	Gentamicin	11.75	7.01	23.40	0.031	33.73	2.04	6.90	36.00	10.70	0.00027

Staphylococcus aureus could be due to the fact that metal complexes penetrate more easily through the bacteria cell wall and destroying it.[37]

3.4.2 Sensitivity patterns of isolates to the tested compounds. The minimum inhibition concentration (MIC) and the diameter of inhibition zone has been determined to be directly proportional to concentration of test compounds. A graph relation of X^2 against the log of concentration was plotted to obtain the intercept of the various drug action. Anti-log of intercept was used to calculate MIC of the tested compounds. Based on this, All the compounds show some form of inhibition for at least two (2) of the bacterial strains studied (Table 2). Compound **L1** shows inhibition of eight (8) bacterial strain out of ten (10) strain studied (Table 2: entry 1). Compound **4** was found to exhibit the most potent *in vitro* anti-bacterial activity with MICs of 1.046 μg mL^{-1} and 0.237 μg mL^{-1} against *Staphylococcus epidermidis* and *Proteus mirabilis* respectively (Table 2: entry 10), while the standard control gentamycin was observed to have MICs ranging from 0.0003 to 33.73 μg mL^{-1} for the ten (10) strains. For the same bacterial strain (*S. epidermidis*), compound **4** performed better compared to gentamicin, MIC of 1.046 μg mL^{-1} and 7.006 μg mL^{-1} respectively (Table 2: entries 10 and 13). The promising antimicrobial effect of **4** may be associated to the palladium metal present since its corresponding ligand **L4** (Table 2: entries 4 and 10) did not perform that well against most of the strains. Interestingly, all the compound were not activity against *S. aureus*.

Generally, the incorporation of palladium metal improve the MIC of the corresponding ligand. For example, Compound **L2** recorded MIC between 4.92 μg mL^{-1} and 34.83 μg mL^{-1} while the corresponding complex **2** recorded MIC between 1.61 μg L^{-1} and 8.46 μg mL^{-1} (Table 2: entries 2 and 8). These trend suggest that the electrophilicity brought about by the dative covalent bonding between the ligands and palladium metal may be responsible for the increase in the inhibition activities at low concentrations of the complexes.

3.4.3 Relative solubility (Log P_{calc} and Experimental Log P) Profile of the tested compounds. Log P values of all the ligands **L1–L6** and complexes **1–6** were calculated to predict their lipophilicity or hydrophilicity. This is one way of determining the extent of their absorption in the human body if formulated as drugs. The Log P of each molecule was compared to the Lipinski Rule which states that molecules or compounds with Log P values of less than five are more likely to show high absorption with less lipophilicity.[38]

The ligands showed moderate to very good log P values hence suggest to have a better absorption; a quality which will affect their ability to stand as variable therapeutics. A close observation showed that, the compounds with sulfonation on the pyrazolyl moiety have better Log P values (**L1** (3.44), **L2** (3.16), **L5** (3.41) and **L6** (3.06)) compared to **L3** and **L4** with Log P of 5.95 and 5.77 respectively. These suggest that compounds **L1**, **L2**, **L5** and **L6** are highly absorbable with optimum lipophilicity and could reach their desired targets easily.

The palladium complexes on the other hand showed higher Log P values of 7.05, 6.69, 7.38 and 6.67 for **1**, **2**, **5** and **6** respectively as well as 12.36 for **3** and 12.00 for **4**. These value are higher compared to the Lipinski rule for their lipophilicity. The Log P of the complexes were found to be about twice that of their respective ligands, a feature that could makes them very good prodrugs capable of delivering double activity during the decomposition of the complexes. From this calculated Log P values suggest that these complexes will show higher activities during *in vivo* studies.

Experimental Log P values were obtained for the compounds. The experimental values confirmed the calculated observation that **L1**, **L2**, **L5** and **L6** (Table S2, ESI†) have more affinity to the lipophilic medium. However, a deviation was observed for the **L3** and **L4** which showed to have high affinity to hydrophilic medium. For example, **L3** was observed to be more hydrophilic with a Log P of −0.83 (Table S2, ESI†) compared to the calculated Log P value of 5.95. A similar trend was observed for the metal complexes where the experimental Log P values for **3** (−0.96) and **4** (−0.72) show affinity for hydrophilic medium while the rest had affinity for the lipophilic medium.

4. Conclusion

Six pyrazolyl sulfonamide ligands as well as their monometallic palladium complexes were synthesized and used as antibacterial agent against 10 bacterial strains. The bacterial strains were

made of Gram positive and Gram negative strain. The MIC values show that the compounds were more active against Gram negative bacteria strain compared to Gram positive strain. The palladium complexes gave improved antibacterial activities compared to their corresponding ligands. Theoretical Log P calculations show that the ligands and complexes could exhibit higher antibacterial activities *in vivo*. However, the experimental Log P value gave a different trend, which shows that compounds with sulfonation only on the phenyl ring make the compounds have high affinity for the hydrophilic medium.

Conflicts of interest

There are no conflicts to declare.

Acknowledgements

We acknowledge the Building A New Generation Of Academics In Africa (BANGA-Africa - Carnegie Corporation of New York), the University of Ghana and the University of Johannesburg for financial support for this project.

References

1 N. D. Friedman, E. Temkin and Y. Carmeli, The negative impact of antibiotic resistance, *Clin. Microbiol. Infect.*, 2016, **22**(5), 416–422, DOI: 10.1016/j.cmi.2015.12.002.
2 M. F. Khan, M. M. Alam, G. Verma, W. Akhtar, M. Akhter and M. Shaquiquzzaman, The therapeutic voyage of pyrazole and its analogs: A review, *Eur. J. Med. Chem.*, 2016, **120**, 170–201, DOI: 10.1016/j.ejmech.2016.04.077.
3 S. G. Kucukguzel and S. Senkardes, Recent advances in bioactive pyrazoles, *Eur. J. Med. Chem.*, 2015, **97**, 786–815.
4 K. Kaur, V. Kumar and G. K. Gupta, Trifluoromethylpyrazoles as anti-inflammatory and antibacterial agents: A review, *J. Fluorine Chem.*, 2015, **178**, 306–326, DOI: 10.1016/j.jfluchem.2015.08.015.
5 S. Malladi, A. M. Isloor, S. K. Peethambar, B. M. Ganesh and P. S. K. Goud, Synthesis and antimicrobial activity of some new pyrazole containing cyanopyridone derivatives, *Der. Pharm. Chem.*, 2012, **4**, 43–52.
6 D. Kaushik, S. A. Khan, G. Chawla and S. Kumar, N′-[(5-chloro-3-methyl-1-phenyl-1*H*pyrazol-4-yl)methylene]2/4-substituted hydrazides: synthesis and anticonvulsant activity, *Eur. J. Med. Chem.*, 2010, **45**, 3943–3949.
7 M. Abdel-Aziz, G. E. A. Abuo-Rahma and A. A. Hassan, Synthesis of novel pyrazole derivatives and evaluation of their antidepressant and anticonvulsant activities, *Eur. J. Med. Chem.*, 2009, **44**, 3480–3487.
8 H. Kumar, D. Saini, S. Jain and N. Jain, Pyrazole scaffold: A remarkable tool in the development of anticancer agents, *Eur. J. Med. Chem.*, 2013, **70**, 248–258.
9 K. M. Dawood, T. M. A. Eldebss, H. S. A. El-Zahabi, M. H. Yousef and P. Metz, Synthesis of some new pyrazole based 1,3-thiazoles and 1,3,4-thiadiazoles as anticancer agents, *Eur. J. Med. Chem.*, 2013, **70**, 740–749.
10 R. C. Khunt, V. M. Khedar, R. S. Chawda, N. A. Chauhan, A. R. Parikh and E. C. Coutinho, Synthesis, antitubercular evaluation and 3D-QSAR study of *N*-phenyl-3-(4- fluorophenyl)-4-substituted pyrazole derivatives, *Bioorg. Med. Chem. Lett.*, 2012, **22**, 666–678.
11 P. Jain, C. Saravanan and S. K. Singh, Sulfonamides: Deserving class as MMP inhibitors, *Eur. J. Med. Chem.*, 2013, **60**, 89–100, DOI: 10.1016/j.ejmech.2012.10.016.
12 CHEMIK. Biological activity and synthesis of sulfonamide derivatives: a brief review. 68. 2014; 620–628.
13 S. J. Sabounchei and P. Shahriary, N-Containing Ag(I) and Hg(II) Complexes: A New Class of Antibiotics, *Curr. Top. Med. Chem.*, 2013, **13**, 3026–3039.
14 E. Budzisz, M. Krajewska and M. Rozalski, Cytotoxic and proapoptotic effects of new Pd(II) and Pt(II)- 489 -complexes with 3-ethanimidoyl-2-methoxy-2*H*-1,2-benzoxaphosphinin-4-ol-2-oxide, Pol. 490, *J. Pharmacol.*, 2004, **56**, 473–478.
15 M. Eslami-Moghadam, A. Divsalar, A. Abolhosseini-Shahrnoy and A. A. Saboury, Synthesis, cytotoxicity assessment, and interaction and docking of novel palladium(II) complexes of imidazole derivatives with human serum albumin, *J. Biomol. Struct. Dyn.*, 2016, **34**, 1751–1762.
16 M. Fanelli, M. Formica, V. Fusi, L. Giorgi, M. Micheloni and P. Paoli, New trends in platinum and palladium complexes as antineoplastic agents, *Coord. Chem. Rev.*, 2016, **310**, 41–79.
17 T. T. H. Fong, C. N. Lok, C. Y. S. Chung, Y. M. E. Fung, P. K. Chow and P. K. Wan, Cyclometalated palladium(II) N-heterocyclic carbene complexes: Anticancer agents for potent in vitro cytotoxicity and in vivo tumor growth suppression, *Angew. Chem., Int. Ed.*, 2016, **55**, 11935–11939.
18 E. Z. Jahromi, A. Divsalar, A. A. Saboury, S. Khaleghizadeh, H. Mansouri-Torshizi and I. Kostova, Palladium complexes: new candidates for anti-cancer drugs, *J. Iran. Chem. Soc.*, 2016, **13**, 967–989.
19 S. Medici, M. Peana, V. M. Nurchi, J. I. Lachowicz, G. Crisponi and M. A. Zoroddu, Noble metals in medicine: latest advances, *Coord. Chem. Rev.*, 2015, **284**, 329–350.
20 J. L. Medina-Franco, M. A. Giulianotti, G. S. Welmaker and R. A. Houghten, Shifting from the single to the multitarget paradigm in drug discovery, *Drug Discovery Today*, 2013, **18**, 495–501.
21 S. Komiya, *Synthesis of Organometallic Compounds: A Practice Guide*, Ed. Board, New York, USA, 1997.
22 E. Goldman and L. H. Green, *Practical handbook of microbiology*, CRC Press, 2015.
23 CLSI (USA). performance standards for antimicrobial susceptibility testing. Approved Standards CLSI, M100-S27. 2017.
24 B. Boney, Principles of assessing bacterial susceptibility to antibiotic using agar well diffusion method, *J. Antimicrob. Chemother.*, 2008, **61**, 129–150.
25 B. Bonev, J. Hooper and J. Parisot, Principles of assessing bacterial susceptibility to antibiotics using the agar diffusion method, *J. Antimicrob. Chemother.*, 2008, **61**, 1295–1301.

26 W. M. Meylan and P. H. Howard, Estimating log *P* with atom/fragments and water solubility with log *P*, *Perspect. Drug Discovery Des.*, 2000, **19**, 67–84.
27 O. S. Attaryan, V. I. Rstakyan and A. G. Hasratyan, Reactions of 3,5-dimethyl-1-phenyl-1*H*-pyrazole with electrophiles, *Russ. J. Gen. Chem.*, 2012, **82**, 1724–1727.
28 *Chemistry of Heterocyclic compounds. In: Chemistry of Heterocyclic compounds*, ed. R. H. Wiley, 1967.
29 R. Koike, K. Higashi, N. Liu, W. Limwikrant, K. Yamamoto and K. Moribe, Structural determination of a novel polymorph of sulfathiazole-oxalic acid complex in powder form by solid-state NMR spectroscopy on the basis of crystallographic structure of another polymorph, *Cryst. Growth Des.*, 2014, **14**, 4510–4518.
30 R. Thakuria, N. K. Nath, S. Roy and A. Nangia, Polymorphism and isostructurality in sulfonylhydrazones, *CrystEngComm*, 2014, **16**, 4681–4690.
31 S. O. Ojwach, I. A. Guzei and J. Darkwa, (Pyrazol-1-ylmethyl)pyridine palladium complexes: Synthesis, molecular structures, and activation of small molecules, *J. Organomet. Chem.*, 2009, **694**, 1393–1399, DOI: 10.1016/j.jorganchem.2008.12.043.
32 C. Amoah, C. Obuah, M. K. Ainooson and A. Muller, Synthesis, characterization and fluorescent properties of ferrocenyl pyrazole and triazole ligands and their palladium complexes, *J. Organomet. Chem.*, 2021, **935**, 121664–121671, DOI: 10.1016/j.jorganchem.2020.121664.
33 F. H. Allen, Research papers -The Cambridge Structural Database: a quarter of a million crystal structures and rising research papers, *Acta Crystallogr., Sect. B: Struct. Sci.*, 2002, **58**, 380–388.
34 M. F. Chellat, L. Raguž and R. Riedl, Targeting Antibiotic Resistance, *Angew. Chem., Int. Ed.*, 2016, **55**, 6600–6626.
35 C. Walsh, Molecular mechanisms that confer antibacterial drug resistance, *Nature*, 2000, **406**, 775–781.
36 P. Dahiya and S. Purkayastha, Phytochemical Screening and Antimicrobial Activity of Some Medicinal Plants against Multi-drug Resistant Bacteria from Clinical Isolates, *Indian J. Pharm. Sci.*, 2012, **74**, 443–450.
37 A. F. Santos, D. F. Brotto, L. R. V. Favarin, N. A. Cabeza, G. R. Andrade, M. Batistote, A. A. Cavalheriro, A. Neves, D. C. M. Rodrigues and A. dos Anjos, Study of the antimicrobial activity of metal complexes and their ligands through bioassays applied to plant extracts, *Rev. Bras. Farmacogn.*, 2014, **24**, 309–315.
38 G. Caron, G. Ermondi and R. A. Scherrer, Lipophilicity, polarity, and hydrophobicity, *Compr. Med. Chem. II*, 2006, **5**, 425–452.

